

REGIONAL PROBLEMS OF GEOCRYOLOGY

TEMPERATURE, COMPOSITION AND AGE OF THE KARA SEA SHELF SEDIMENTS  
IN THE AREA OF THE MARRE-SALE GEOCRYOLOGICAL STATION

V.A. Dubrovin, L.N. Kritsuk, E.I. Polyakova\*

*All-Russian Research Institute of Hydrogeology and Engineering Geology (VSEGINGEO),  
Zeleny Village, Moscow Oblast, 142452, Russia; dva946@yandex.ru*

*\* Lomonosov Moscow State University, Department of Geography,  
1 Leninskie Gory, Moscow, 119991, Russia; ye.polyakova@mail.ru*

The paper presents results of the study of the uppermost 20 m-thick layer of the near-Yamal shelf bottom sediments, penetrated in May 2014 by two VSEGINGEO boreholes equipped with LPC loggers, with an aim of the temperature regime dynamics monitoring in the nearshore bottom sediments, both for the research purposes and in as much as the data add value to the forthcoming hydrocarbon resource development on the Russian continental shelf. On the basis of the temperature variation observations during three summer months of 2014, it has been established that marine silty clays and aleurites composing the bottom sediment section, represent relict frozen deposits subjected to cryogenic metamorphism in the subaerial exposure environment. Diatom assemblages occurring in aleurite and clayey deposits consist exclusively of the marine extinct species typical of the Early Eocene *Pyxilla gracilis* diatom zone. A modern marine sublittoral diatom assemblage is found inhabiting the sands of the upper part of the onshore borehole section.

*Shelf, borehole, bottom sediments, monitoring, autonomous measuring complex, temperature regime, diatom assemblages*

INTRODUCTION

The Marre-Sale Permafrost Station (geocryological permanent study area) staffed by the VSEGINGEO researchers was established in 1978 on western coast of the Yamal Peninsula, in the area shared with the weather station of the same name, which has been used for continuous observations since 1914. The Marre-Sale Permafrost Station (PS) being a data source of the Russia's long-term permafrost monitoring and one of the few base station for long-term observations of the permafrost evolution in the context of climate changes, serves as a basic observation point area for permafrost studies applicable to the resource development in the Arctic areas of the West Siberian petroleum region [Dubrovin, 2009; Krupoderov and Dubrovin, 2012].

Its location in close proximity to the polar meteorological station favors the use of weather observation sequences, which contributes to a better representativity of both its observations proper and predictive estimations of the area-specific variations of the permafrost parameters. Geological-geocryological section of the Marre-Sale area, especially in its upper, the most ice-rich part, serves as a reference for essentially large part of western and central Yamal, the Kara Sea shelf, and Baidaratskaya Bay areas.

Geocryological observations at the Marre-Sale PS have been run for 37 years and therefore are found highly reliable in estimations of the background (global, regional) alterations of the thermal state of permafrost, reflecting its sensitivity to altered meteorological parameters.

At the time the Marre-Sale PS was established, one of the pressing scientific challenges and a rationale for its operations was to study the seasonal and annual dynamics of perennially frozen deposits (PFD) and their temperature regime variations. By the end of the XX<sup>th</sup> century, geocryological conditions of the permafrost table had been studied fairly well to a depth of 10–12 m [Pavlov *et al.*, 1996]. From 1995 to 2009, four wells equipped with a universal automated measuring complex "LPC data logger" were drilled in the area of the Marre-Sale PS under different landscape and geological conditions at depths ranging from 60 to 110 m [Dubrovin *et al.*, 1996]. The system allowed to obtain fairly accurately depicted temperature regime of the permafrost strata over a long time-period. Beginning from 2000, the loggers became an indispensable element of the equipment in all newly drilled wells, which includes the 16 wells drilled to a depth from 20–30 m to 110 m and shown in Fig. 1.

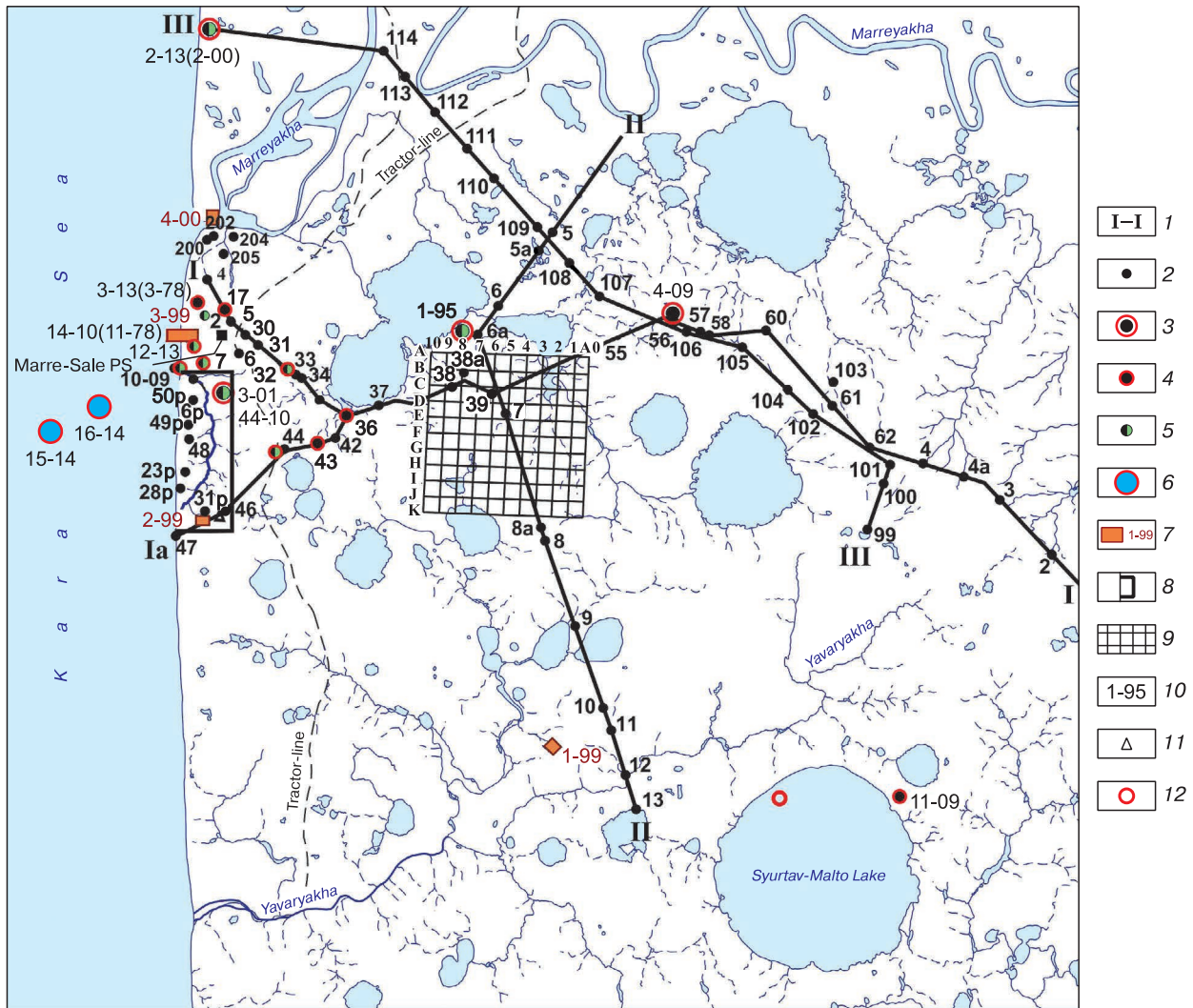


**Fig. 1. Layout scheme of observation points of the VSEGINGEO stationary.**

1 – Profiles: I, II – geotechnical-geocryological, III – monitoring observations. Boreholes: 2 – geotechnical-geocryological, 3 – deep, 4 – with logger, 5 – with seismic logging, 6 – on the shelf. Test areas: 7 – observation sites, 8 – semicircular morphostructure, 9 – “Kvadrat” testing ground. 10 – well No. and the year of drilling; 11 – bench mark; 12 – logger on the lake bottom surface.

The long-term monitoring observations resulted in a fairly profound analysis of the main features of temperature variations (annual and multiyear) in the coastal area of the southern Yamal Peninsula, with the observations materials regularly processed and research results and findings published and presented at conferences [Dubrovin et al., 1996; Kritsuk and Dubrovin, 2000, 2006; Dubrovin and Kritsuk, 2011; Krupoderov and Dubrovin, 2012].

The study of the near-Yamal shelf permafrost interval was challenged primarily by the lack of any data on temperature regime of the bottom sediments at depths of the offshore installations, required in the context of the forthcoming development of hydrocarbon fields in the area. Therefore, two wells dedi-

cated for sediment temperature regime monitoring with a depth of 20 m below the sea floor were spudded in the Marre-Sale PS area in May 2014 as part of the state-commissioned technical assignment to “Rosnedra”.

### RESEARCH RESULTS

The first offshore well (BH 15-14) was drilled on the –5.0 m isobath line at a distance of 860 meters from the shore, the second well (BH 16-14) on –4.0 m isobaths, 500 meters from the shore (Fig. 1). The wells were spudded from the ice layer (with thickness 1.8–2.3 m) with the “Sterkh” drilling rigs and UB-SHM-20 system. After the drilling was completed the wells were cased with viewing metal pipes (57 mm in

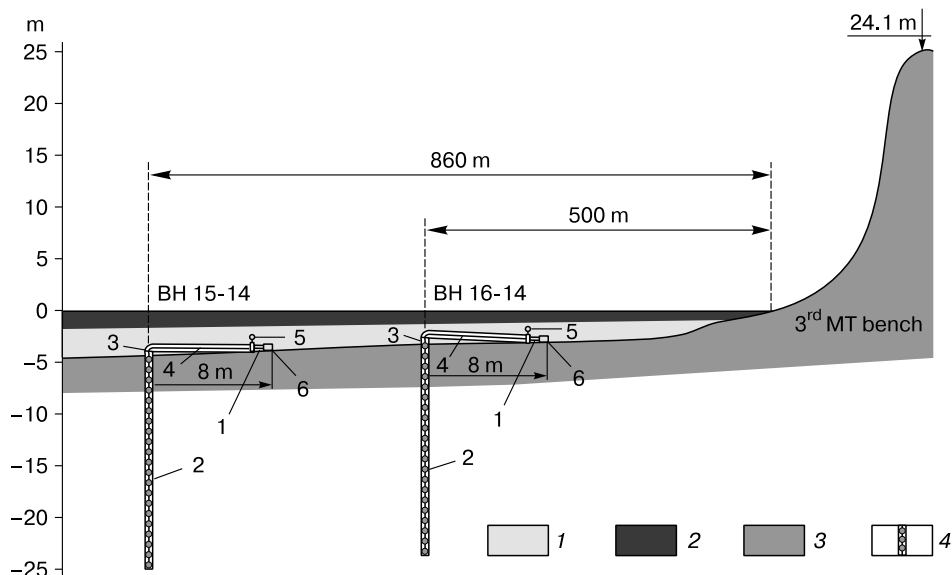


**Fig. 2. Safety instrument system of the VSEGINGEO boreholes on the Kara Sea shelf.**

1 – LPC logger; 2 – well casing; 3 – safety clamp; 4 – pipe junction (flexible pipe); 5 – float; 6 – load. 1 – seawater; 2 – ice; 3 – onshore ground, offshore bottom deposits; 4 – boreholes with thermistor string.

diameter) and equipped with the LPC-F measuring systems.

Temperature sensors are arranged in the thermistor chain with 1 m spacing, beginning from the sediment surface and deeper down to the bottom hole (Fig. 2). In the bottom layer, the crown of the tube is equipped with 8 m-long flexible hose (pipe) 80 mm in diameter with special anchor weights, to preclude its

surfacing. The wells positions were strictly tied to the land area by various means, including a GPS-navigator, theodolite, shore ranges of various design (Fig. 3).

Subsequent to the construction of wells on the seafloor, an operation test was run for the observation post. During the week to follow, the temperature measurements were regularly taken (until they reached constant values, thus signaling about stabili-

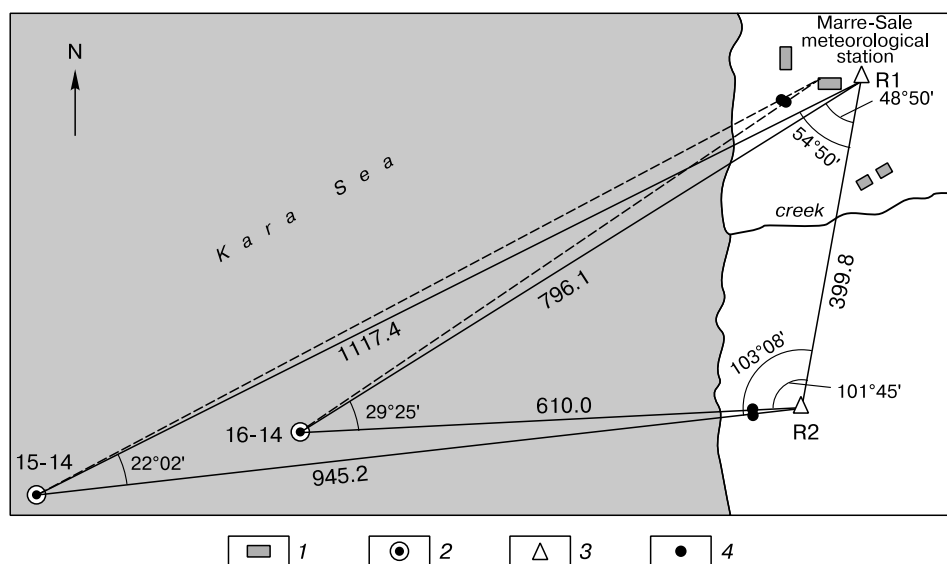


**Fig. 3. Georeferencing plan of the offshore VSEGINGEO boreholes.**

1 – Marre-Sale meteorological station; 2 – borehole spudded in 2014 and its No.; 3 – reference point and its No.; 4 – range marks.

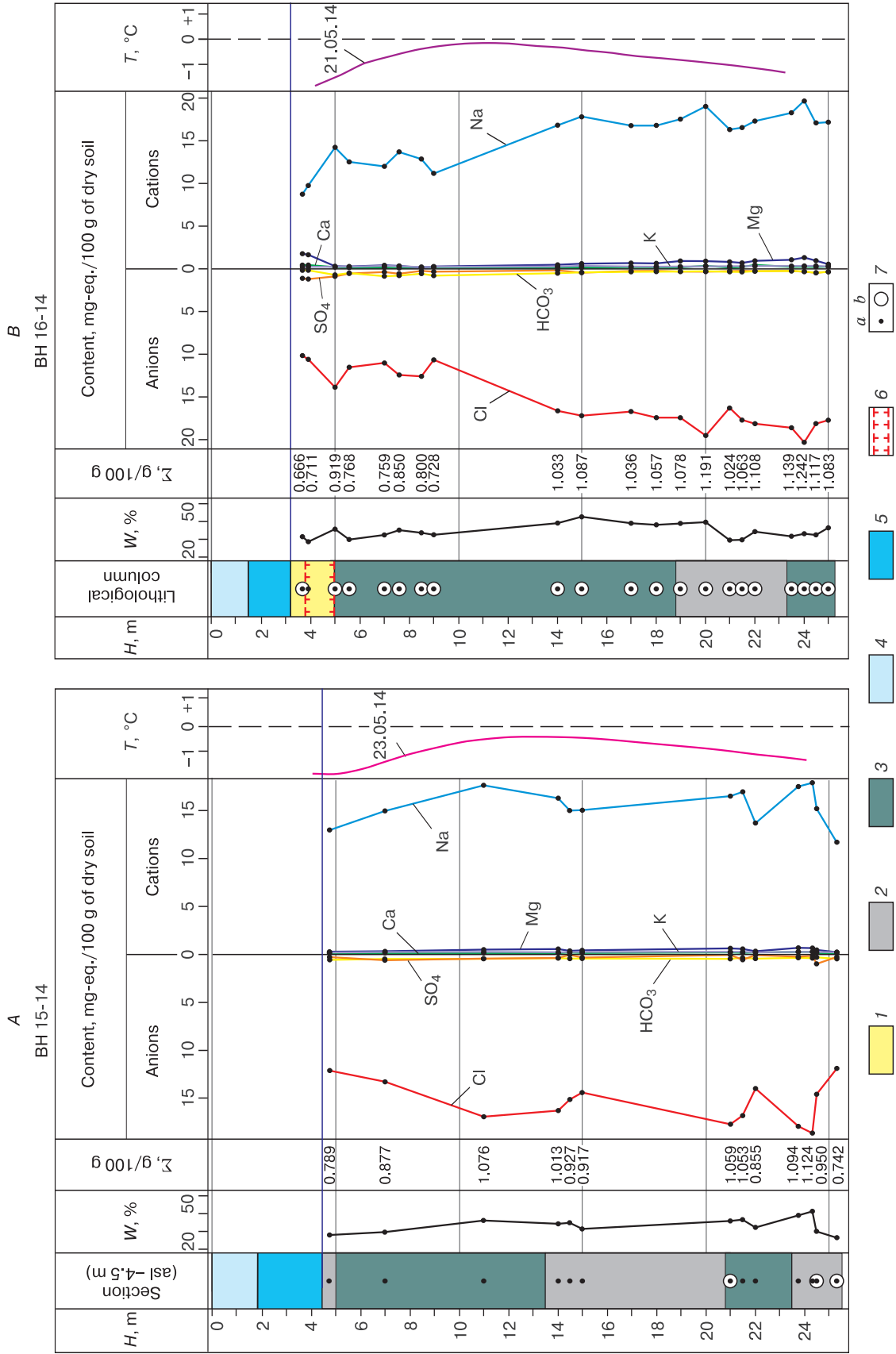


**Fig. 4. Geological sections of the offshore VSEINGEEO wells.**

A – BH 15-14; B – BH 16-14; 1 – sand; 2 – silty clay; 3 – aleurite; 4 – sea ice; 5 – seawater; 6 – boundaries of frozen deposits; 7 – core sampling points; a – for lab tests, b – for diatom analyses. H – depth; W – moisture (water) content of ground; Σ – TDS sum; T – ground temperature.

zation of the temperature regime, which had been disturbed by the drilling), and primary data were collected from the gauges.

**Temperature of the near-Yamal shelf bottom sediment.** Already first temperature records from the VSEGINGEO wells drilled on the shelf, provided new insights into specificity of the temperature regime of bottom sediment in the vicinity of the Marre-Sale PS.

Fig. 4 represents geological sections of the two wells with the first temperature measurements (as of May 2014). The curves analysis has shown that the temperature of the 20 m thick sedimentary strata range between  $-0.1...-0.3$  and  $-1.8...-2.0$  °C.

Subsequent to the destruction of ice cover in August 2014, the temperature was remeasured in the periphery well (BH 15-14). Flexible pipe of the well lay-head with the incorporated LPC-F measuring gauge were lifted up to the surface and secured to the boat. The observations data (gauges readings) over the period spanning from May through August 2014 (Fig. 5) were taken with the use of a laptop PC.

The measurements taken at different times displayed a dense graph, which is indicative of high measurement accuracy (Fig. 5, A). Fig. 5, B shows a clearly visible gradually decreasing trend in temperature gradient at depths in the range of 6–14 m. The analysis of Fig. 5, A, B, allowed to infer that the bottom sediment temperature has been affected by the warming observable over the last decade, which was reflected in the records from the onshore wells (Fig. 5, C). Given the analysis of the year-round temperature variations in the offshore wells drilled are scheduled for 2015, this conjecture is anticipated to be confirmed or refuted therewith.

Fig. 5, A, B show the zero isotherm dynamics in the bottom sediment of BH 15-14. In the period from June, 12 to 22 it was aligned with the seafloor surface, which is primarily associated with the presence and gradual destruction of the sea ice, given that the thawing of the frozen top of the section is also possible. At this, in the period from 19 May to 20 August, temperature of silty clays decreased from  $-0.6$  to  $-0.8$  °C at a depth of 6 m, and from  $-0.3$  to  $-0.7$  °C, at a depth of 8 m. The seafloor temperature varied from  $-1.9$  to  $+4.0$  °C in BH 15-14 during the observation period. At a depth of 20 m below the seafloor, the sediment temperature was  $-1.4$  °C in BH 15-14 and  $-1.3$  °C in BH 16-14.

**Geology of the shelf.** The wells were drilled on the seafloor using an auger-type drill system. Sediment samples for laboratory tests were taken from the auger blade (at preset borehole torpedoing depth) from each of the layers (with changing lithologies) or 1 m above (given the sediments composition is homogeneous). The sampling and initial descriptions of

cores in parallel with the hole making was done by E.A. Slagoda, Dr in geol.-mineral. sci (Institute of Earth Cryosphere (IKZ SB RAS), Tyumen).

The bottom sediment samples preserved at the VSEGINGEO laboratories were analyzed for particle size distribution, water and physical properties, along with the determination of the chemical composition of water extraction. Table 1 and 2 provide data on ion concentration, the amount of salt (TDS) and laboratory marking of cores. Both granulometric and lithological compositions were correlated with the laboratory analyses. When marking the core samples, the VSEGINGEO analysts referred to the standard geotechnical documentation [*GOST 25100*]. The marine sediments of similar composition, containing more than 30 % of clay particles are called silty (or sandy) clays. Sediments with less clay particles are called aleurites (silts) [*Great... Encyclopedia, 1976, p. 29*].

The seafloor sediments in BH 15-14 are composed of silty clay of varying degrees of plasticity (from soft and fluid-plastic to fluid), with interbedding of silts – in the 14.5–15.0, 21.0–23.5, 25.0–25.3 m intervals – of flowing consistency (Table 1). In the 4.0–4.5 and 24.3–25.3 m intervals, the sediments are dense, and probably in the frozen state, without visible inclusions of ice (according to the description by E.A. Slagoda). Under the in-situ conditions the sediments color is bluish-gray or bluish-black; in the dry state, their color is light gray or chocolate brown.

The granulometric composition of silty clays is as follows: sand – 10 to 25 % (most particles are 0.10–0.05 mm in diameter); silt particles – from 40 to 50 %; clay – from 32 to 45 %. Moisture content varies in the range from 28 to 42 %. The composition and properties of the sediments in BH 16-14 and 15-14 differ essentially (Table 2). Given that BH 16-14 is located closer to the shore, it is affected by the longshore currents from the mouth of the Marre-Yaha river<sup>1</sup>.

Fine, well-washed sands occur at the 0–1.8 m depth interval (below the seafloor surface), with the content of 0.25–0.1 mm fraction found higher than 90 %. The overlying water-saturated sand occurring at a depth of 0.5 m is frozen, strongly cemented by ice (Fig. 6, d). Silty clays of varying consistency from fluid to low-plastic were encountered in the interval between 5 and 17 m, and aleurites of flowing consistency are interlayered with silty clay (fluid-plastic) in the 24.5–25.0 m interval within the 17–25 m depth range.

Lab tests results showed the following granulometric composition of silty clays in BH 16-14: sand particles (with size 0.10–0.05 mm) – from 6 to 13 %; silt particles – from 40 to 60 %; clay – from 35 to 50 %. The aleurites display an increasing content of sand particles (up to 25–40 %), with the clay content

<sup>1</sup> Over the span of three months the wellhead of BH 16-14 was found surfaced with a layer of sand.

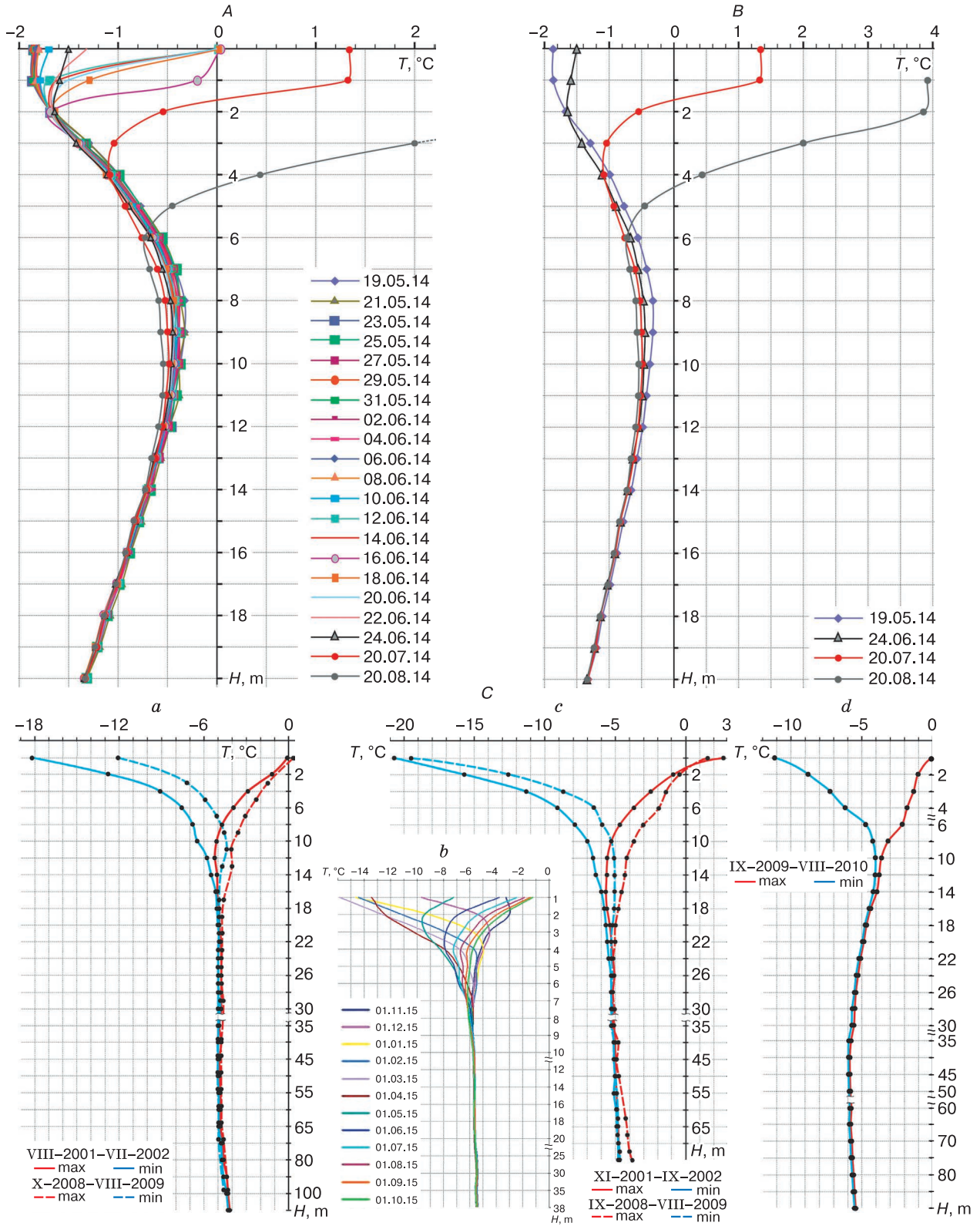


**Рис. 5. Sediment temperature in wells drilled in the area of the VSEGINGEO permafrost station Marre-Sale.** A – BH 15-14, May–August 2014; B – BH 15-14, in different times; C – extreme temperatures in deep wells in the vicinity of the permafrost station: a – 1-95; b – 2-00; c – 3-01, d – 4-09 (cf. Fig. 1).

Table 1. Lithologic composition and salinity of bottom sediments in BH 15-14

Depth, m	Lithologic composition of sediments	Kurlov Formula (%-eq.)	Sum of ions, g/100 g	pH	Genetic markers of seawater		
					Na/K	Na/Cl	SO <sub>4</sub> /Cl
4.5	Clay loam, heavy, hard-plastic	$\frac{\text{Cl } 93.5 \text{ HCO}_3 \text{ 4.3 SO}_4 \text{ 2.2}}{\text{Na } 95.5 \text{ Mg } 2.1 \text{ K } 1.5 \text{ Ca } 0.9}$	0.789	7.6	63.7	1.02	0.02
7.0	Clay loam, heavy, w/silt grade particles, soft-plastic	$\frac{\text{Cl } 92.5 \text{ HCO}_3 \text{ 3.3 SO}_4 \text{ 4.2}}{\text{Na } 95.3 \text{ Mg } 2.2 \text{ K } 1.5 \text{ Ca } 1}$	0.877	7.4	63.3	1.03	0.05
11.0	Clay loam, heavy, w/silt grade particles, fluid-plastic	$\frac{\text{Cl } 95.1 \text{ HCO}_3 \text{ 2.5 SO}_4 \text{ 2.4}}{\text{Na } 94.9 \text{ Mg } 2.8 \text{ K } 1.5 \text{ Ca } 0.8}$	1.076	7.5	63.3	1.0	0.026
14.0	Idem	$\frac{\text{Cl } 95.7 \text{ HCO}_3 \text{ 2.2 SO}_4 \text{ 2.1}}{\text{Na } 94.6 \text{ Mg } 3.3 \text{ K } 1.3 \text{ Ca } 0.8}$	1.013	7.5	72.8	0.99	0.02
14.5	Clay loam, light-textured, fluid	$\frac{\text{Cl } 97 \text{ HCO}_3 \text{ 2.8 SO}_4 \text{ 0.2}}{\text{Na } 94.7 \text{ Mg } 2.4 \text{ K } 1.6 \text{ Ca } 1.3}$	0.927	7.5	59.2	0.98	0.002
15.0	Clay loam, heavy, w/silt grade particles, soft-plastic	$\frac{\text{Cl } 95.7 \text{ HCO}_3 \text{ 2.2 SO}_4 \text{ 2.1}}{\text{Na } 94.6 \text{ Mg } 3.3 \text{ K } 1.3 \text{ Ca } 0.8}$	0.917	7.4	72.8	0.99	0.021
21.0	Clay loam, light-textured, w/silt grade particles, fluid	$\frac{\text{Cl } 97.2 \text{ HCO}_3 \text{ 2.5 SO}_4 \text{ 0.3}}{\text{Na } 93.6 \text{ Mg } 3.6 \text{ K } 1.6 \text{ Ca } 1.2}$	1.059	7.6	58.5	0.96	0.006
21.5	Idem	$\frac{\text{Cl } 95 \text{ SO}_4 \text{ 3 HCO}_3 \text{ 2}}{\text{Na } 94.2 \text{ Mg } 3.2 \text{ K } 1.6 \text{ Ca } 1}$	1.053	7.3	58.9	0.99	0.032
22.0	»	$\frac{\text{Cl } 96.5 \text{ HCO}_3 \text{ 3 SO}_4 \text{ 0.5}}{\text{Na } 94.8 \text{ Mg } 2.3 \text{ K } 1.5 \text{ Ca } 1.4}$	0.855	7.5	63.2	0.98	0.005
23.5	Clay loam, heavy, w/silt grade particles, fluid	$\frac{\text{Cl } 96.8 \text{ HCO}_3 \text{ 2 SO}_4 \text{ 1.2}}{\text{Na } 93.3 \text{ Mg } 3.7 \text{ K } 1.5 \text{ Ca } 1.5}$	1.094	7.2	62.2	0.96	0.012
24.3	Idem	$\frac{\text{Cl } 97.3 \text{ HCO}_3 \text{ 2 SO}_4 \text{ 0.7}}{\text{Na } 93.5 \text{ Mg } 3.5 \text{ K } 1.5 \text{ Ca } 1.5}$	1.124	7.5	62.3	0.96	0.007
25.0	Clay loam, light-textured, w/silt grade particles, soft-plastic	$\frac{\text{Cl } 91.6 \text{ SO}_4 \text{ 6.2 HCO}_3 \text{ 2.2}}{\text{Na } 94.5 \text{ Mg } 3 \text{ K } 1.6 \text{ Ca } 0.9}$	0.950	6.8	59.1	1.03	0.022
25.3	Clay loam, heavy, w/silt grade particles, hard-plastic	$\frac{\text{Cl } 94.1 \text{ HCO}_3 \text{ 3.7 SO}_4 \text{ 2.2}}{\text{Na } 95 \text{ Mg } 2 \text{ K } 1.9 \text{ Ca } 1.1}$	0.742	6.9	50.0	1.01	0.023
1	Ocean water	$\frac{\text{Cl } 90.2 \text{ SO}_4 \text{ 9.3 HCO}_3 \text{ 0.5}}{\text{Na } 77 \text{ Mg } 17.9 \text{ Ca } 3.5 \text{ K } 1.6}$	35008*	7.5	48.0	0.1	0.86
2	Seawater, 100 m from the shore	$\frac{\text{Cl } 91 \text{ SO}_4 \text{ 9}}{\text{Na } 77 \text{ Mg } 18 \text{ Ca } 3 \text{ K } 2}$	30.223	7.2	38.5	0.1	0.85
3	River water in the Marre-Yakha river estuary	$\frac{\text{Cl } 88 \text{ SO}_4 \text{ 10 HCO}_3 \text{ 2}}{\text{Na } 77 \text{ Mg } 18 \text{ Ca } 3 \text{ K } 2}$	1.474	6.2	38.5	0.11	0.87
4	Idem, 4.6 km from the estuary	$\frac{\text{Cl } 82 \text{ HCO}_3 \text{ 12 SO}_4 \text{ 6}}{\text{Na } 71 \text{ Mg } 22 \text{ Ca } 6 \text{ K } 1}$	0.480	7.7	71.0	0.07	0.87

\* A Reference Book for Hydrogeologists, 1962, p. 170.

declining (down to 19–29 %); silt grade particle portion has grown from 40 to 55 %. Moisture content of sand is 30 %, whereas that of aleurite varies in the range of 29–39 %, and accounts for 30–43 % in silty clay.

A high content of opoka-like material being a distinctive feature of silty clays in both wells, they tend to be superplastic – when rolled out, they form a very thin ribbon and stick to the lips – which is characteristic of Paleocene clay deposits of Western Siberia.

The seafloor sediments in both wells are saline, with salt content ranging from 0.8–1.2 g per 100 g of soil in BH 15-14, and from 0.7 to 1.2 g per 100 g of soil in BH 16-14. Given that salinization of the sediment is dictated by seawater, Cl<sup>-</sup> ions and Na<sup>+</sup> largely predominate (Fig. 4, Tables 1, 2). However, ionic ratio in the sediments of both wells differ from the that of inherent to seawater. Almost all the tested samples of bottom sediment (except for sands in BH 16-14) have displayed increased content of Cl<sup>-</sup> (95–96 % eq.) ions, and, especially, Na<sup>+</sup> (93–95 % eq.),

Table 2. Lithologic composition and salinity of bottom sediments in BH 16-14

Depth, m	Lithologic composition of sediments	Kurlov Formula (%-eq.)	Sum of ions, g/100 g	pH	Genetic markers of seawater		
					Na/K	Na/Cl	SO <sub>4</sub> /Cl
3.3	Fine sand	$\frac{\text{Cl } 88.8 \text{ SO}_4 \text{ 9.7 HCO}_3 \text{ 1.5}}{\text{Na } 78.1 \text{ Mg } 16 \text{ Ca } 3.9 \text{ K } 2}$	0.666	7.4	39.0	0.88	0.11
3.9	Idem	$\frac{\text{Cl } 88.7 \text{ SO}_4 \text{ 9.9 HCO}_3 \text{ 1.4}}{\text{Na } 80.8 \text{ Mg } 13.7 \text{ Ca } 3.6 \text{ K } 1.9}$	0.711	7.4	46.7	0.91	0.11
5.0	Clay loam, heavy, w/silt grade particles, soft-plastic	$\frac{\text{Cl } 89.7 \text{ SO}_4 \text{ 5.7 HCO}_3 \text{ 4.6}}{\text{Na } 95 \text{ Mg } 2.0 \text{ Ca } 1.4 \text{ K } 1.6}$	0.919	7.5	59.4	1.06	0.03
5.5	Clay loam, heavy, w/silt grade particles, hard-plastic	$\frac{\text{Cl } 91.7 \text{ SO}_4 \text{ 4.4 HCO}_3 \text{ 3.9}}{\text{Na } 94.9 \text{ Mg } 2.2 \text{ K } 1.9 \text{ Ca } 1}$	0.768	7.5	49.9	1.03	0.05
7.0	Clay loam, heavy, w/silt grade particles, soft-plastic	$\frac{\text{Cl } 89.9 \text{ HCO}_3 \text{ 7 SO}_4 \text{ 3.1}}{\text{Na } 92.9 \text{ Mg } 3.2 \text{ K } 2.7 \text{ Ca } 1.2}$	0.759	7.5	34.4	1.03	0.033
7.5	Clay loam, heavy, w/silt grade particles, fluid-plastic	$\frac{\text{Cl } 90 \text{ HCO}_3 \text{ 5.8 SO}_4 \text{ 4.2}}{\text{Na } 94.8 \text{ Mg } 2.4 \text{ K } 2.1 \text{ Ca } 0.7}$	0.850	7.6	45.1	1.05	0.05
8.5	Idem	$\frac{\text{Cl } 93.9 \text{ HCO}_3 \text{ 4.4 SO}_4 \text{ 1.7}}{\text{Na } 95.9 \text{ Mg } 1.1 \text{ K } 1.6 \text{ Ca } 1.4}$	0.800	7.6	59.9	1.02	0.02
9.0	Clay loam, heavy, w/silt grade particles, soft-plastic	$\frac{\text{Cl } 90.5 \text{ HCO}_3 \text{ 6.7 SO}_4 \text{ 2.8}}{\text{Na } 94.2 \text{ Mg } 2.3 \text{ K } 2 \text{ Ca } 1.5}$	0.728	7.8	47.1	1.04	0.03
14.0	Clay loam, heavy, w/silt grade particles, fluid	$\frac{\text{Cl } 96 \text{ HCO}_3 \text{ 3 SO}_4 \text{ 1}}{\text{Na } 94.8 \text{ Mg } 2.7 \text{ K } 1.5 \text{ Ca } 1}$	1.033	7.6	63.2	0.98	0.001
15.0	Idem	$\frac{\text{Cl } 95.3 \text{ SO}_4 \text{ 2.5 HCO}_3 \text{ 2.2}}{\text{Na } 94.1 \text{ Mg } 3.2 \text{ K } 1.9 \text{ Ca } 0.8}$	1.087	7.4	49.5	0.99	0.026
17.0	Clay loam, light-textured, w/silt grade particles, fluid	$\frac{\text{Cl } 96.6 \text{ HCO}_3 \text{ 2 SO}_4 \text{ 1.4}}{\text{Na } 93.6 \text{ Mg } 3.8 \text{ K } 1.5 \text{ Ca } 1.1}$	1.036	7.3	62.4	0.97	0.014
18.0	Idem	$\frac{\text{Cl } 97 \text{ HCO}_3 \text{ 1.8 SO}_4 \text{ 1.2}}{\text{Na } 94 \text{ Mg } 3.6 \text{ K } 1.4 \text{ Ca } 1}$	1.057	7.3	67.1	0.97	0.012
19.0	»	$\frac{\text{Cl } 96.5 \text{ HCO}_3 \text{ 1.8 SO}_4 \text{ 1.7}}{\text{Na } 92.8 \text{ Mg } 4.8 \text{ Ca } 0.9 \text{ K } 1.5}$	1.078	7.3	61.9	0.96	0.017
20.0	»	$\frac{\text{Cl } 96.9 \text{ SO}_4 \text{ 1.7 HCO}_3 \text{ 1.4}}{\text{Na } 92.5 \text{ Mg } 4.4 \text{ Ca } 1.7 \text{ K } 1.4}$	1.191	7.1	66.1	0.95	0.016
21.0	Clay loam, light-textured, w/silt grade particles, fluid-plastic	$\frac{\text{Cl } 96.4 \text{ HCO}_3 \text{ 2 SO}_4 \text{ 1.6}}{\text{Na } 92.8 \text{ Mg } 4.6 \text{ Ca } 0.9 \text{ K } 1.7}$	1.024	7.3	54.6	1.0	0.017
21.5	Clay loam, light-textured, w/silt grade particles, fluid	$\frac{\text{Cl } 96.7 \text{ HCO}_3 \text{ 2 SO}_4 \text{ 1.3}}{\text{Na } 93.3 \text{ Mg } 3.9 \text{ Ca } 1.1 \text{ K } 1.7}$	1.063	7.8	54.9	0.96	0.013
22.0	Idem	$\frac{\text{Cl } 97 \text{ SO}_4 \text{ 1.5 HCO}_3 \text{ 1.5}}{\text{Na } 91 \text{ Mg } 5 \text{ Ca } 2.4 \text{ K } 1.6}$	1.108	7.3	56.9	0.94	0.015
23.5	»	$\frac{\text{Cl } 97.4 \text{ HCO}_3 \text{ 1.3 SO}_4 \text{ 1.3}}{\text{Na } 91.8 \text{ Mg } 5.4 \text{ K } 1.6 \text{ Ca } 1.2}$	1.139	7.2	57.4	0.94	0.013
24.0	»	$\frac{\text{Cl } 97 \text{ SO}_4 \text{ 1.6 HCO}_3 \text{ 1.4}}{\text{Na } 91.2 \text{ Mg } 6.1 \text{ Ca } 1.2 \text{ K } 1.5}$	1.242	7.2	60.8	0.94	0.016
24.3	Clay loam, heavy, w/silt grade particles, fluid-plastic	$\frac{\text{Cl } 95.1 \text{ HCO}_3 \text{ 2.5 SO}_4 \text{ 2.4}}{\text{Na } 91.8 \text{ Mg } 5.1 \text{ K } 1.8 \text{ Ca } 1.3}$	1.117	7.8	51.0	0.96	0.025
25.0	Clay loam, light-textured, w/silt grade particles, fluid	$\frac{\text{Cl } 96.1 \text{ HCO}_3 \text{ 2 SO}_4 \text{ 1.9}}{\text{Na } 94 \text{ Mg } 3 \text{ K } 1.6 \text{ Ca } 1.4}$	1.083	7.6	58.8	0.98	0.02

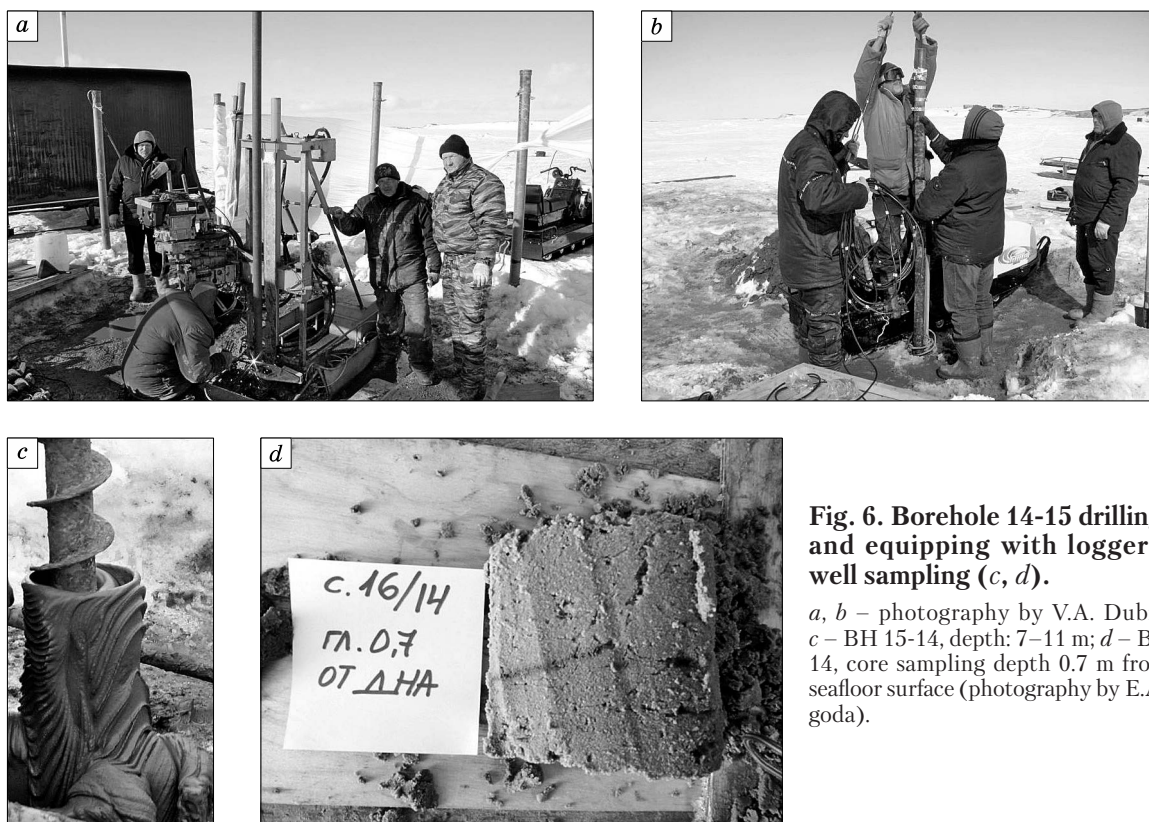


**Fig. 6. Borehole 14-15 drilling (a) and equipping with logger (b), well sampling (c, d).**

*a, b* – photograph by V.A. Dubrovin; *c* – BH 15-14, depth: 7–11 m; *d* – BH 16-14, core sampling depth 0.7 m from the seafloor surface (photography by E.A. Slagoda).

which is indicative of the cryogenic metamorphism of pore solution [Anisimova, 1981; Fotiev, 2009]. The content of  $Mg^{2+}$  ions is anomalously low;  $SO_4^-$  ions concentration is essentially less than in seawater (it's only in the BH 16-14 sand that sulfate-ion content is found close to that of seawater). Unlike the composition of modern seawater, all the tested samples (38 pcs.) contain  $HCO_3^-$  ions (up to 3–4 % eq. in BH 15-14 and 6–7 % eq. in BH 16-14).

Along with the laboratory tests results for the bottom sediment composition and salinity, Tables 1 and 2 provide the calculated genetic markers of sea water as the ratios of basic ions. Their values for oceanic and sea waters are provided in the bottom part of Table 1. When compared, the three indicators values obtained for the offshore wells with the ambient sea and ocean waters displayed their essential difference, as well as great variability in the borehole sections.

It stands to reason that such a situation (aggravated by chaotic variations of the amount of salts (TDS) through the section depths) can be solely accounted for cryogenic metamorphism of the marine sediments. At this, the persistent presence of ions in them suggests that the marine sediments composing the sections of both wells were subjected to cryogenic metamorphism under subaerial conditions.

Hypothetical salts contained in the sediments and determined by the Anisimova technique [1981],

are shown in Table 3. Analysis of the data revealed that salts of continental origin – magnesium bicarbonate and potassium and sodium sulfate – persist in the sections of the offshore wells, indicating that the studied marine strata is well-washed by fresh water (lake-, river-, or groundwater).

The above-discussed specific salt composition and superplasticity of the shelf bottom sediment provide a rationale for suggesting their pre-Pleistocene age and the erosion nature of the geological section of the shelf. This hypothesis is corroborated by the results of multiyear investigations of the of the Kara Sea coastal dynamics, carried out by the VSEGIN-GEO researchers at the Marre-Sale PS [Kritsuk, 2010; Kritsuk et al., 2014].

Analysis of the repeated aerial photography and satellite imagery using GIS technology revealed that over 44 years (1969–2013), the annual (mean multi-annual) retreat of the base of the Kara Sea coastal cliffs in the vicinity of Marre-Sale village constitute 1.5 m, i.e. 150 meters over a century. Thus, some 300–350 years ago the coast may have been shifted 450–500 m from the present position, and 800–900 m – as late as 500–600 ya. This means that the boreholes spudded in 2014 at the bottom of the shelf exposed the ancient subaerial sections.

Silty clays, similar to those encountered on the shelf bottom, are exhibited on the day surface in the

Table 3. Hypothetic salts in the near-Yamal shelf bottom sediments

Sampling depth, m	NaCl	MgCl <sub>2</sub>	Na <sub>2</sub> SO <sub>4</sub>	MgSO <sub>4</sub>	CaSO <sub>4</sub>	NaHCO <sub>3</sub>	MgHCO <sub>3</sub>	CaHCO <sub>3</sub>	KCl	KSO <sub>4</sub>	KHCO <sub>3</sub>
Ocean water	77.6	10.7	–	6.8	2.5	–	–	0.8	1.6	–	–
Water in the Marre-Yakha rv. estuary	76.7	10.3	–	7.1	3.0	–	5.0	1.5	1.6	–	1.0
<i>BH 16-14</i>											
3.3	78.1	10.7	–	5.3	3.9	–	–	–	–	0.5	1.0
3.9	80.8	7.9	–	5.8	3.6	–	–	–	–	0.5	1.4
5.0	89.7	–	5.3	0.4	–	–	1.6	1.4	–	–	1.6
8.5	93.9	–	1.7	–	–	0.3	1.1	1.4	–	–	1.6
9.0	90.5	–	2.8	–	–	0.9	2.3	1.5	–	–	2.0
19.0	92.8	3.7	–	1.1	0.6	–	–	0.3	–	–	1.5
20.0	92.5	4.4	–	–	1.7	–	–	–	–	–	1.4
21.0	92.8	–	–	1.0	0.6	–	–	0.3	–	–	1.7
24.0	91.2	5.8	–	0.3	1.2	–	–	–	–	0.1	1.4
25.0	94.0	2.1	–	0.9	1.0	–	–	0.4	–	–	1.6
<i>BH 15-14</i>											
4.5	93.0	2.0	2.0	0.1	–	–	–	0.9	–	–	1.5
7.0	92.5	–	2.8	1.4	–	–	0.8	1.0	–	–	1.5
11.0	94.9	0.2	–	2.4	–	–	0.2	0.8	–	–	1.5
14.0	94.6	1.1	–	2.1	–	–	0.1	0.8	–	–	1.3
14.5	94.7	2.3	–	0.1	0.1	–	–	1.2	–	–	1.6
15.0	94.6	1.1	–	2.1	–	–	0.1	0.8	–	–	1.3
21.0	93.6	3.6	–	–	–	–	–	1.2	–	0.3	1.3
21.5	94.2	0.8	–	2.4	–	–	–	1.0	–	0.6	1.0
22.0	94.8	1.7	–	0.5	–	–	0.1	1.4	–	–	1.5
23.5	93.3	3.5	–	0.2	–	–	–	1.5	–	1.0	0.5
24.3	93.5	3.5	–	–	0.4	–	–	1.1	0.3	–	1.2
25.0	91.6	–	2.9	3.0	0.3	–	–	0.6	–	–	1.6
25.3	94.1	–	0.9	1.3	–	–	0.7	1.1	–	–	1.9

coastal outcrops in the areas of the Marre-Yakha and Yavar-Yakha rivers estuaries. They are commonly associated with the outcrops of ground ice or traces of its presence in the past: large thermocirques, giant “cemetery mounds” (baidzharakhs), deep ravines and gullies, clay pebbles, etc. [Kritsuk, 2010].

Most of the researchers studying the Marre-Sale sections believe these clays to be deep-sea sediments of Pleistocene age [Zubakov and Levkovskaya, 1968; Danilov, 1986; Gataullin, 1991; Streletskaya et al., 2009; Slagoda et al., 2012]. However, there exist other viewpoints on the origin and age of the deposits composing the Marre-Sale coastal outcrops. In that way, F.A. Kaplyanskaya and V.D. Tarnogradskii [1982] believe the Mare-Sale Formation to have formed in the lacustrine basin at the end of the Paleogene and early in Neogene. A similar inference was made by E.I. Polyakova on the basis of the study of the diatom assemblages of argillaceous sediments, composing the central part of a large semicircular morphostructure with melting ground ice, exposed on the Kara Sea coastal bluffs [Polyakova and Danilov, 1989]. Accord-

ing to V.N. Gataullin [1991], the Marre-Sale coastal deposits with ground ice bodies formed in the Pra-Ob river delta. The ancient age (pre-Pleistocene) of the Marre-Sale deposits is ultimately corroborated by the VSEGINGEO long-term comprehensive research conducted in the coastal zone, along with the study of the section, penetrated by the offshore wells [Kritsuk, 2010].

BH No. 15-14 and No. 16-14 were drilled opposite the semicircular radial concentric morphostructure 0.4 km in width – about 1 km stretch along the coast (Fig. 1, 7), which holds icy bodies of different size and morphology (layers, lenses, laccoliths and veins), up to 10–15 m thick. The ice thawing processes have been observed by different researchers for over 40 years. This morphostructure has previously been studied in detail by the authors [Kritsuk and Dubrovina, 2000, 2006; Kritsuk, 2010; Kritsuk et al., 2014].

The VSEGINGEO researchers carried out comprehensive research within its area back in 1986, deploying geophysical surveys, which included: electrical profiling (to delimit horizontal boundaries) and

vertical sounding (delineating vertical boundaries); drilling out extreme points on the electrical profiles (to depths between 12 and 15 m); cryolithological study of drill-cores from the boreholes and coastal outcrops, as well as massive sampling of ground ice and surface waters, to determine their chemical and isotopic composition [Kritsuk, 2010].

In 2001, BH 3-01 was drilled onshore to a depth of 84 m in the marginal part of the semicircular morphostructure at a distance of 300 meters from the coastline (the elevation of wellhead is 21.5 m, the height above the gully bottom is 15 m) (Fig. 7). The well was spudded in October 2001 using a bar-rigged system, and initially ran dry, but from a depth of 13.7 m the drilling progressed with washing by saline mud. The BH 3-01 section is shown in Fig. 8, and its full description is provided in the paper [Kritsuk, 2010].

Cryogenic structure of the section of onshore BH 3-01 bears the evidence of secondary-intrasoil genesis of ice inclusions (fractured type), diagenetically transformed aquatic (stratified) deposits and, consequently, their ancient age. The specific characteristics include: high density and low ice content of clays and sands (except contacts with ice bodies); predominance of cryogenic textures of massive type; rare inclusions of inclined and vertical icy veinlets and laminae in the horizontally stratified argillaceous and sandy deposits (supported by vertical stratification of ice body, laid bare in the 4.9–12.0 m interval); the presence of layers of fine-shattered silty clays contacting directly with ice layers.

Spatial distribution of the salinity (TDS) components in BH 3-01 is closely related to the sediment material composition, and therefore to the origin of the designated layers (Fig. 8), which accounts for the marine sediments represented by only saline clays occurring deeper than 38.2 m there. In composition, they are identical to silty clays, penetrated by the offshore wells. The clays salinity pattern in BH 3-01 is found similar to that recorded in boreholes No. 15-14 and 16-14. TDS content varies in the range of 0.76–1.07 g per 100 g soil, with  $\text{Cl}^-$  and  $\text{Na}^+$  ions greatly prevailing in the ionic composition.

The clays were probably subjected to washing with fresh water, since they tend to be overlain by the aquatic (lacustrine and river (?)) [Gataullin, 1991]) stratified sandy-argillaceous deposits. Much like for the deposits from the offshore wells, records of BH 3-01 bear the evidence of the presence of  $\text{Na}_2\text{SO}_4$  and  $\text{Mg}(\text{HCO}_3)_2$  salts and show violent oscillation of the marine genetic markers, similar to those considered above, in the shelf section (Tables 1, 2). The marine genesis of the strata was determined in the course of microstructural studies by the particle size distribution analysis method developed by A.V. Surkov [Streletskaya et al., 2009].

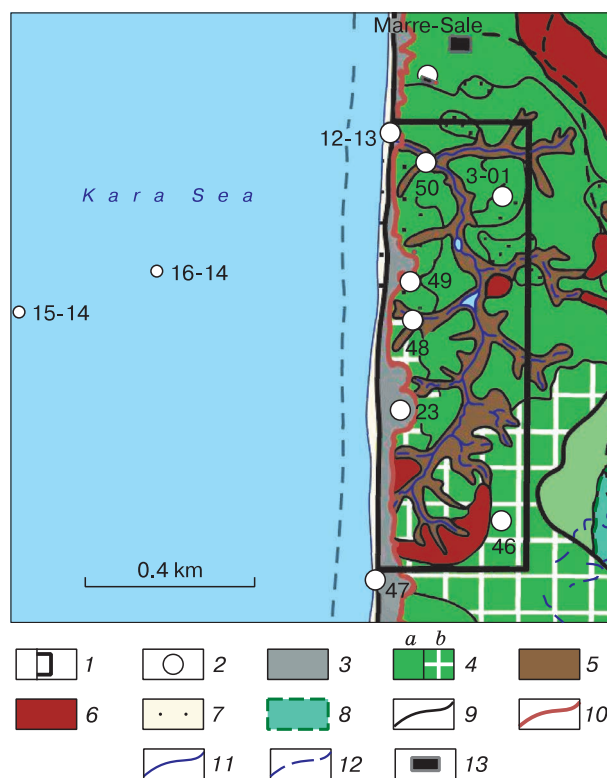


**Fig. 7. Semicircular morphostructure on the Kara Sea shore (a fragment of geocryological zoning map for the Marre-Sale permafrost station area).**

1 – the VSEGINGEO integrated land data acquisition site in 1986; 2 – borehole and its No.; 3 – thermal abrasion shoreface; 4 – types of geocryological sections: *a* – near slope crests with patches of sand, *b* – idem, with polygonal fracture network; 5 – gullies and ravines; 6 – polygonal peat bog; 7 – sea beach; 8 – drained lakes (khasyreys); 9 – boundary between geomorphological levels; 10 – seashore crest in 2013; 11 – shoreline in 2013; 12 – idem, in 1969; 13 – Marre-Sale weather station.

The origin and age of the rhythmically layered argillaceous strata penetrated by BH 3-01 in the 13.7–29.4 m interval were determined to be the lacustrine and Miocene, respectively, by E.I. Polyakova in the diatom studies (from core samples of the coastal outcrops) [Polyakova and Danilov, 1989]. The sands encountered at a depth of 29.4–38.0 m are likely to be coastal-marine and analogous to those in BH 16-14.

Age determination of the bottom sediments is possible only subsequent to the detailed diatom analysis.

**Research results of diatom assemblages.** To carry out the study of diatom assemblages, 23 samples of the bottom sediment were selected from the cores recovered in boreholes drilled on the shelf in 2014: three from BH 15-14 and 20 pcs from BH 16-14. The studied samples are shown in the section of the wells drilled (Fig. 4, legend 7). The samples were processed

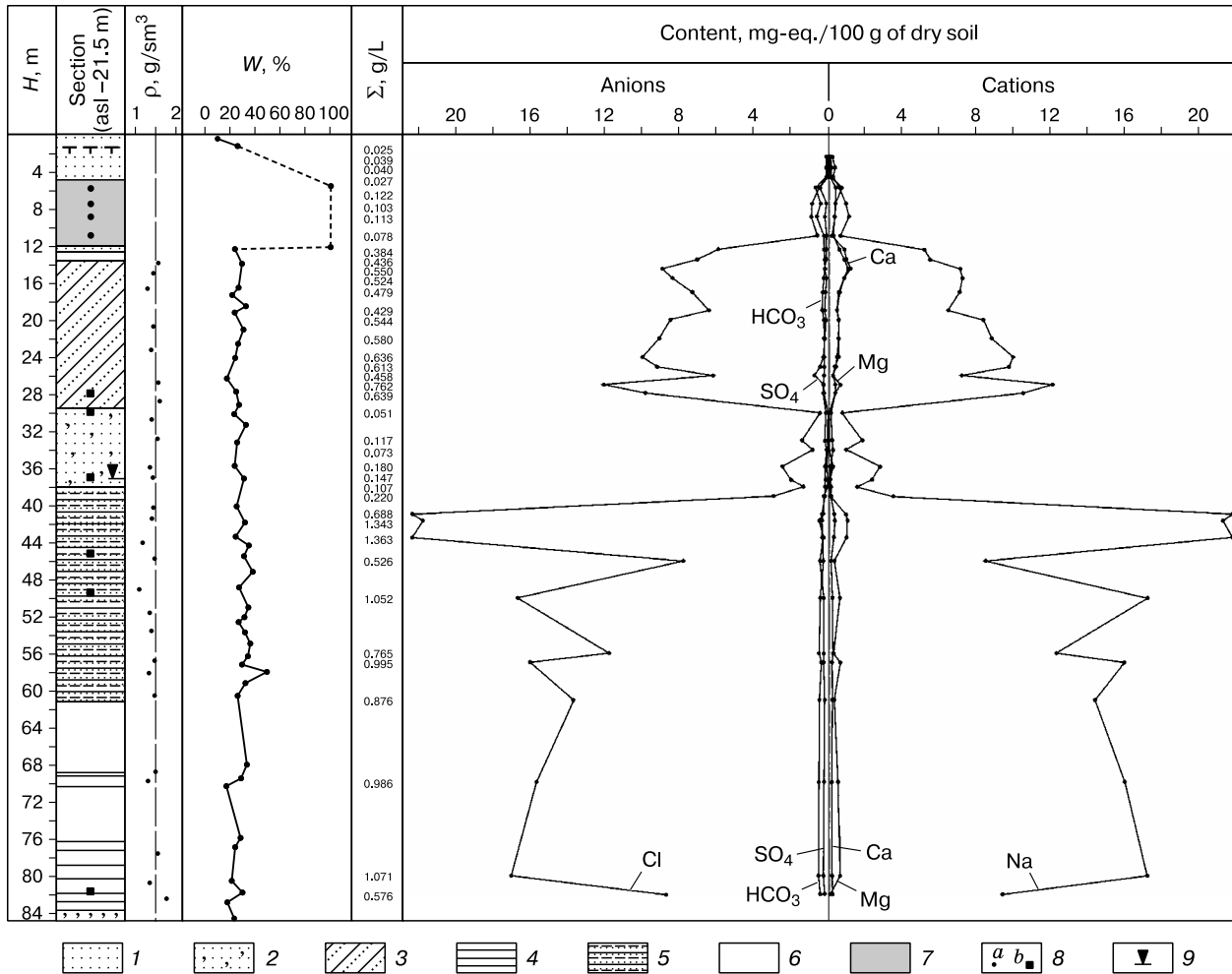


**Fig. 8. Geological section and salt composition of soils in BH 3-01.**

1 – fine sand; 2 – silty sand; 3 – sandy silt loam; 4 – silty clay; 5 – interbedding of clay, aleurite and silty sand; 6 – penetration w/o core sampling; 7 – ice; 8 – core sampling points: *a* – for hydrochemical and ice isotope composition analyses, *b* – for mineral composition of soil; 9 – ground water (cryopeg).  $\rho$  – average soil density. Other legends cf. Fig. 4.

by the Battarbee method [Battarbee, 1973] at the Institute of Oceanology of the Russian Academy of Sciences, and then studied by E.I. Polyakova (MSU).

The diatom analysis of sediments showed abundant and taxonomically diverse diatom assemblages, represented for the most part by the extinct Paleogene species. The present-day diatom assemblage has thus far been identified only in fine sands of the uppermost layers in BH 16-14 (0–1.8 m from the sea floor), where it is represented by brackish-water and marine diatom species (*Diploneis smithii* (Brébisson) Cleve, *Thalassiosira hyperborea* (Grunow) Hasle, *Navicula digitoradiata* (Gregory) Ralfs), typical for the present-day and Quaternary sediments of the coastal areas of the Kara Sea shelf subjected to freshening [Polyakova, 1997, 2003].

A major part of the investigated sections of the wells (BH 16-14: the 5.0–25.0 m sediment interval; BH 15-14: the 21.0–24.5 m interval), represented by silty clays and aleurites contained valves of only extinct species of the marine diatoms, which belong to Paleogene fossil species. The Paleogene diatom valves are well preserved and present in high abundance. Not any remains of either Quaternary diatoms or silicoflagellates were found in these deposits.

The established assemblages are predominated by the extinct species of the marine tychoipelagic diatoms genera *Paralia*, *Anuloplicata*, *Hyalodiscus*, with sponge spicules fairly abundant, which is indicative of the sea basin being relatively shallow. The identified diatom assemblages in the two wells are characterized by a great diversity of species (ca.30), which include those observed in high abundance marked by *Pyxilla*

*gracilis* Tempère et Forti, *Grunowiella gemmata* (Grunow) Van Heurck, *Coscinodiscus payeri* Grunow, *Pyxidicula arctica* (A. Schmidt) Strelnikova et Nikolaev, *Pyxidicula moelleri* (Grunow) Strelnikova et Nikolaev, *Coscinodiscus decrescens* Grunow, *Pyxidicula punctata* (Jousé) Strelnikova et Nikolaev, *Hemiaulus polymorphus* Grunow, *Pseudopodosira westii* (W. Smith) Sheshukova–Poretzskaya et Glezer, *Anuloplicata ornata* (Grunow) Glezer, *Paralia sulcata* var. *siberica* (Grunow) Grunow, *Hyalodiscus radiatus* (O'Meara) Grunow. In general, these complexes typify the Lower Eocene diatom *Pyxilla gracilis* zone of the extratropical Paleogene scale [Glezer, 1974; Strelnikova, 1992], identified in the deposits of upper subformation of the Lyulinvor suite in many parts of Western Siberia and in eastern slope of the Northern Urals [Strelnikova, 1992; Oreshkina et al., 2008; Akhmet'ev et al., 2010; Oreshkina, 2012].

It should be noted that, diatom valves assigned to the Paleogene marine flora are commonly distributed in the form of redeposited microfossils in the northern West Siberia – in the Quaternary deposits of various origins [Polyakova, 1997; Schkabichevskaya, 1984]. Their redeposition is evidenced by the environmental incompatibility of species with the genesis of the surrounding deposits, for example, those represented by alluvial-lacustrine facies. The inconsistency in the age of diatoms represented by species from the known stratigraphic range of distribution in the Cenozoic would also serve a signature of their redeposition in Quaternary marine sediments. Moreover, the valves of redeposited diatoms are usually poorly preserved (partially broken up or dissolved).

The studies of the seafloor diatom-bearing sediments exposed in the offshore VSEGINGEO boreholes near Cape Marre-Sale, bear the evidence of the ancient marine origin of the sediments (at least, those occurring to a depth of –5 m isobath line). The abundant and taxonomically diverse diatom assemblages, including index-species of the Paleogene zonal scale allowed a sufficiently high accuracy in establishing the stratigraphic position of both assemblages and the surrounding sediment (the Lower Eocene *Pyxilla gracilis* zone).

## CONCLUSIONS

The study of the topmost 20-meter thick sediment strata on the near-Yamal shelf on the basis of data from two VSEGINGEO boreholes dedicated for temperature monitoring of the sea bottom sediments (spudded in May 2014), permitted the following inferences.

Equipping the boreholes with the autonomous automatic measuring gauges based on “Logger-4PC” made possible the direct measurements of the bottom sediment temperature and in three months time to take the readings for the purpose of temperature

monitoring as often as twice a day. During the observation period (three months), the seafloor temperature has changed from –1.9 to +4.0 °C in BH 15-14. At a depth of 20 m below the sea bottom, the sediment temperature was –1.4 °C in BH 15-14, and –1.3 °C in BH 16-14. During the observation period the temperature decreased by 0.1–0.4 °C in the 6–14 m interval of BH 15-14.

The data were obtained on the composition and properties of the near-Yamal shelf bottom sediments, which revealed that the studied strata is composed of silty clays and aleurites of plastic or fluid consistency, which had been exposed to multiyear-cooling. The sedimentary strata represents by itself a relict permafrost affected by cryogenic metamorphism under sub-aerial conditions.

It is the first time that diatom assemblages have been studied in detail on the Kara Sea shelf, as part of regional studies. It was established that in 22 cores diatoms from argillaceous deposits (sampled from both wells) are represented by the extinct marine species characteristic of the Lower Eocene diatom *Pyxilla gracilis* zone and upper member of the Lyulinvor Formation in Western Siberia and in the Eastern Urals. The present-day subtidal marine diatom assemblage was identified only in one sample (attributed to fine sand) from the uppermost part of the onshore well section.

## References

- Akhmet'ev, M.A., Zaporozhets, N.I., Yakovleva, A.I., 2010. Comparative analysis of the marine Paleogene sections and biota of Western Siberia and Arctic. *Stratigr. Geol. Korrelyatsii*. (6), V. 18, pp. 78–103.
- Altovskii, M.E. (Ed.), 1962. A Reference Book for Hydrogeologist. Gosgeoltekhizdat, Moscow, 616 pp. (in Russian)
- Anisimova, N.P., 1981. Cryohydrochemical Characteristics of the Frozen Zone. Nauka, Novosibirsk, 152 pp. (in Russian)
- Battarbee, R.W., 1973. A new method for estimation of absolute microfossil numbers, with reference especially to diatoms. *Limnol. Oceanogr.*, V. 18, pp. 647–654.
- Gataullin, V.N., 1991. Marre-Sale Formation in Western Yamal – deposits of the Pra-Ob delta, in: Commission for the study of the Quaternary Period, *Bulletin*, (60). Moscow, pp. 53–61. (in Russian)
- Glezer, Z.I., 1974. Eocene diatoms, in: *Diatomaceous Algae in the USSR Area*. Nauka, Leningrad, V. I, pp. 109–142. (in Russian)
- GOST 25100, 2011. Interstate Standard. Soils. Classification. Standart, Moscow, 36 pp. (in Russian)
- Great Soviet Encyclopedia, 1976. *Bolshaya Sovetskaya Entsiklopedia*, Moscow, V. 25, 600 pp. (in Russian)
- Danilov, I.D., 1986. Dislocations in frozen, containing tabular ice, Pleistocene deposits of the northern West Siberia, in: *Formation of Frozen Rocks and Prediction of Cryogenic Processes*. Nauka, Moscow, pp. 28–41. (in Russian)
- Dubrovina, V.A., 2009. Geocryological studies in the subsurface management and use system: challenges, tasks, problem solution. *Razvedka i Okhrana Nedr*, No. 9, 36–42.

- Dubrovin, V.A., Karavanova, M.E., Kulikov, A.I., Fedoseev, A.V., 1996. Automated measurement systems and geocryological database in the GMGS (state monitoring of geological environment) system. Proc. of the First conf. of Russian geocryologists. Moscow University Press, Moscow, V. 2, pp. 457–465.
- Dubrovin, V.A., Kritsuk, L.N., 2011. Estimation of frozen rocks temperature regime dynamics in the Marre-Sale area, on the basis of monitoring observations. Proc. of the Fourth conf. of Russian geocryologists. Moscow University Press, Moscow, V. 2, pp. 236–243.
- Fotiev, S.M., 2009. Cryogenic Metamorphism of Rocks and Ground Waters (conditions and results). Geo Publishers, Novosibirsk, 280 pp. (in Russian)
- Kaplyanskaya, F.A., Tarnogradskii, V.D., 1982. Glacial landforms in the area of Marre-Sale village, Yamal Peninsula. Tr. VSEGEL, NS, V. 319, pp. 77–84.
- Kritsuk, L.N., 2010. Ground Ice of Western Siberia. Nauchnyi Mir, Moscow, 350 pp. (in Russian)
- Kritsuk, L.N., Dubrovin, V.A., 2000. Ground Ice Bodies and Cryogenic Processes in the Marre-Sale area (Western Yamal). Hydrogeological, geotechnical and geocryological investigations: Collection of VSEGINGEO papers, Geoinformmark, Moscow, pp. 14–25. (in Russian)
- Kritsuk, L.N., Dubrovin, V.A., 2006. Some results of the study of the Marre-Sale area geocryological conditions in deep wells, in: Theory and Practice of Estimating the State of the Earth Cryosphere. Proc. of the Intern. Conf. Izd-vo Neftegazovy un-t, Tyumen, V. I, pp. 247–251. (in Russian)
- Kritsuk, L.N., Dubrovin, V.A., Yastrebova, N.V., 2014. Some results of integrated study of the Kara seashore dynamics in the Marre-Sale meteorological Station area, with the use of GIS-technologies. Kriosfera Zemli XVIII (4), 59–69.
- Krupoderov, V.S., Dubrovin, V.A., 2012. Problematic aspects of investigations and resource development of the Arctic permafrost, in: Proc. of the Tenth Conf. on Permafrost. Pechatnik, Tyumen, V. 3, pp. 275–279. (in Russian)
- Oreshkina, T.V., 2012. Signatures of Early Eocene climatic optimum (EECO) in biosilicious sediments of Western Siberia and adjacent areas. Proc. of the XV<sup>th</sup> All-Russian micropaleontological conf. "Modern Paleontology". GIN, Moscow, pp. 355–358.
- Oreshkina, T.V., Yakovleva, A.I., Aleksandrova, G.H., 2008. Direct Correlation of the boreal Paleogene zonal schemes by diatoms and dinocysts (from Well No. 19-U records, Ust-Man'ya vill., eastern slope of the Northern Urals). Novosti paleontologii i stratigrafii. Supplement to "Geologia i Geofizika", V. 49, (10–11), pp. 347–350.
- Pavlov, A.V., Dubrovin, V.A., Kharitonov, L.P., 1996. Experimental study of soils thermal regime in the Arctic regions of Western Siberia, in: Proceed. of the 1<sup>st</sup> Conf. of Russian Geocryologists, Moscow University Press, Moscow, Book 1, pp. 310–320.
- Polyakova, E.I., 1997. The Eurasian Arctic Seas During the Late Cenozoic. Nauchyi Mir, Moscow, 145 pp. (in Russian)
- Polyakova, E.I., 2003. Diatom assemblages in surface sediments of the Kara Sea (Siberian Arctic) and their relationship to oceanological conditions, in: Siberian river run-off in the Kara Sea. Characterisation, quantification, variability and environmental significance / Stein, R., Fahl, K., Fütterer, D.K., Galimov, E.M., Stepanets, O.V. (Ed.). Elsevier, N.Y., pp. 375–400.
- Polyakova, E.I., Danilov, I.D., 1989. The Miocene of the Far North of Western Siberia. Doklady Akademii Nauk SSSR, V. 308, (2), pp. 428–431.
- Skabichevskaya, N.A., 1984. Middle-Late Quaternary Diatoms of the Fore-Yenisei North. Nauka, Moscow, 157 pp. (in Russian)
- Slagoda, E.A., Opokina, O.L., Rogov, V.V., Kurchatova, A.N., 2012. Structure and origin of massive ground ice in Upper Pleistocene – Holocene deposits of Cape Marre-Sale (Western Yamal). Kriosfera Zemli XVI (2), 9–22.
- Streletskaia, I.D., Shpolyanskaya, N.A., Kritsuk, L.N., Surkov, A.V., 2009. Cenozoic deposits of the Western Yamal and problem of their origin. Vestnik MGU, Ser. 5, Geografia, No. 3, 50–57.
- Strelnikova, N.I., 1992. Peleogene Diatomaceous Algae. Izd. St.-Peterb. un-ta, St. Petersburg, 311 pp. (in Russian)
- Zubakov, V.A., Levkovskaya, G.M., 1968. Stratigraphy of the recent deposits in the low reaches of the Ob river, in: Quaternary Geology and Geomorphology of Siberia. Nauka, Novosibirsk, Pt. 1, pp. 62–83. (in Russian)

*Received January 28, 2015*